GEOPHYSICAL RESEARCH LETTERS, VOL. 34, L02108, doi:10.1029/2006GL028254, 2007

Mass and electron densities in the inner magnetosphere during a prolonged disturbed interval

R. S. Grew,[1] F. W. Menk,[1] M. A. Clilverd,[2] and B. R. Sandel[3]

Received 22 September 2006; revised 6 December 2006; accepted 13 December 2006; published 24 January 2007.

[1] The equatorial plasma density and composition at $L = 2.5$ were studied during an extended disturbed interval using field line resonance measurements (yielding plasma mass density), naturally and artificially stimulated VLF whistlers (electron number density) and IMAGE EUV observations (plasmapause position and line-of-sight He^+ intensity). During the storm the plasmapause moved to $L < 2.5$ and at least one density notch and drainage plume formed. These features were evident in all the data sets for some days. One notch extended from 2.4–4.5 R_E and spanned <4 hours in MLT. Plume mass and electron densities were enhanced by a factor of about 3. In the plasmasphere and plasmatrough the H^+: He^+: O^+ composition by number was ~82:15:3. However, just outside the plasmapause the O^+ concentration exceeded 50%, suggesting the presence of an oxygen torus.

Citation: Grew, R. S., F. W. Menk, M. A. Clilverd, and B. R. Sandel (2007), Mass and electron densities in the inner magnetosphere during a prolonged disturbed interval, *Geophys. Res. Lett.*, *34*, L02108, doi:10.1029/2006GL028254.

1. Introduction

[2] The inner magnetosphere is often regarded as containing a well-ordered population of co-rotating cold dense plasma. However, recent imaging of this region by the Extreme Ultraviolet (EUV) instrument on the IMAGE spacecraft [*Sandel et al.*, 2000] has shown that a variety of density irregularities such as localized depletions and drainage plumes may form, and that the plasmasphere may rotate at as low as 44% of corotation [*Gallagher et al.*, 2005; *Sandel et al.*, 2003].

[3] Multi-instrument studies during times of low and moderate magnetic activity [e.g., *Dent et al.*, 2003; *Clilverd et al.*, 2003] have demonstrated how ground and satellite-based techniques can be combined to investigate temporal variations in the plasmaspheric ion and electron density. Such observations may be compared with empirical model predictions of the plasmaspheric density and composition as a function of magnetic activity [e.g., *Young et al.*, 1982] and radial distance [*Berube et al.*, 2005]. However, such models may not describe unusually disturbed geomagnetic conditions well.

[4] This paper reports a coordinated multi-instrument study of plasma density and composition at $L = 2.5$ during an extended disturbed interval. The techniques used involve (i) measuring the resonant frequency of geomagnetic field lines, allowing the total mass density in the equatorial plane to be estimated; (ii) determining the equatorial electron density through the dispersion of naturally and artificially stimulated field-aligned VLF whistler mode waves; and (iii) estimating the He^+ column abundance and hence the equatorial He^+ density using the EUV instrument on the IMAGE spacecraft.

2. Interval and Method

[5] We focus on the disturbed interval that extended from 30 Sep. to 8 Oct. 2002 (days 273–281; average daily maximum $K_p = 6_o$). This was not a typical storm. Following a sudden commencement at 0916 UT on 30 Sep., Dst reached −176 nT on 1 Oct., and fell below −100 nT on several of the following days (see Figure 2 in section 3). The IMF B_z at the ACE spacecraft (~1 hour upstream of the Earth) turned strongly northward ~12 UT on 30 Sep., then strongly southward ~3 UT on 1 Oct., northward again around 00 UT on 3 Oct., then southward again around 12 UT that day. The solar wind density at ACE exceeded 40 H^+/cc during the first B_z northward interval on 30 Sep.

[6] The eigenfrequencies of geomagnetic field lines were evaluated with the cross-phase and related methods [*Menk et al.*, 2004, and references therein] using closely spaced magnetometer pairs. Field line resonance (FLR) frequencies scaled from whole-day dynamic spectra and discrete individual static spectra were used to calculate mass densities in the equatorial plane assuming an R^{-3} radial density dependence and a dipolar magnetic field. Magnetometer data came from the SAMNET and IMAGE arrays in the UK and Scandinavia (~85–120° magnetic longitude (MLON)) and from Vernadsky (65°S, 64°W geog.) and Rothera (67.5°S, 68.1°W geog.) on the Antarctic peninsula (midpoint $L = 2.62$; ~4.4° MLON). To facilitate comparison with electron densities (below), the Antarctic mass densities were then scaled to $L = 2.5$ assuming an R^{-3} radial dependence.

[7] VLF whistler data were obtained using two different techniques. Naturally occurring whistlers (triggered by lightning) recorded at Halley (67°S, 27°W geog., $L = 4.67$) were analyzed to provide electron density estimates [e.g., *Clilverd et al.*, 2003]. We also used the VLF Doppler technique, employing whistler mode signals stimulated by a VLF transmitter near the Rothera conjugate point in Maine, USA. These signals were analyzed after *Clilverd et al.* [2003, and references therein]. Densities from the two techniques were then scaled (by R^{-3}) to $L = 4$ and $L = 2.5$ respectively, these being the average footprints of the whistler ducts.

[1]School of Mathematical and Physical Sciences, University of Newcastle, Callaghan, New South Wales, Australia.
[2]British Antarctic Survey, Cambridge, UK.
[3]Lunar and Planetary Laboratory, University of Arizona, Tucson, Arizona, USA.

0094-8276/07/2006GL028254$05.00

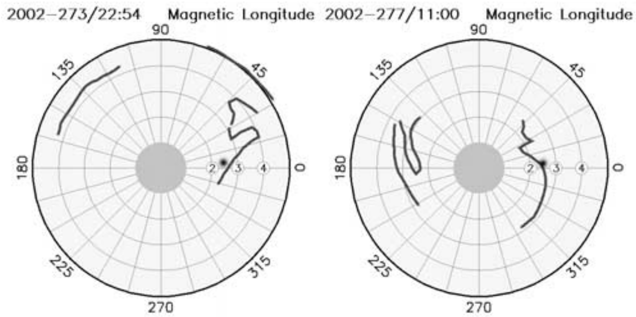

Figure 1. IMAGE EUV tracer images during the storm (left) initial phase and (right) recovery phase. Grey dots indicate L = 2.5 Antarctic ground station projections; concentric circles represent radial distances from 2 R_E (L = 2) to 5 R_E (L = 5); and labels on the 5 R_E perimeter denote magnetic longitude.

[8] IMAGE EUV observations are presented below in two forms. Tracer plots show the location of the plasmapause based on He^+ image intensities mapped to the equatorial plane, following *Goldstein et al.* [2003]. Further examples of such plots are given by *Sandel et al.* [2003] and *Goldstein et al.* [2003]. Equatorial He^+ densities at L = 2.5 were also estimated following the method described by *Clilverd et al.* [2003] and *Gallagher et al.* [2005].

3. Observations

[9] Figure 1 shows the IMAGE EUV plasmapause location at 2254 UT on 30 Sep. (Figure 1, left) and 1100 UT on 4 Oct. 2002. The first image (and others not presented for this day) show that over the 30–160° MLON (20–05 MLT) sector the plasmapause was beyond L = 4 prior to the storm commencement, but with an Earthward excursion to L < 3 at <30° MLON, and the formation of a drainage plume near L = 5. A well-defined narrow plume is also visible in Figure 1 (right), 4 days later, near 180° MLON (18 MLT). The visible plasmapause was now at $L \leq 3$, while a localized density cavity near 20° MLON extended to L < 2. Following *Sandel et al.* [2003] we refer to such a localized density depletion as a 'notch.' A plume was visible in EUV images at least until 7 Oct., although it is likely that more than one plume formed during the interval considered.

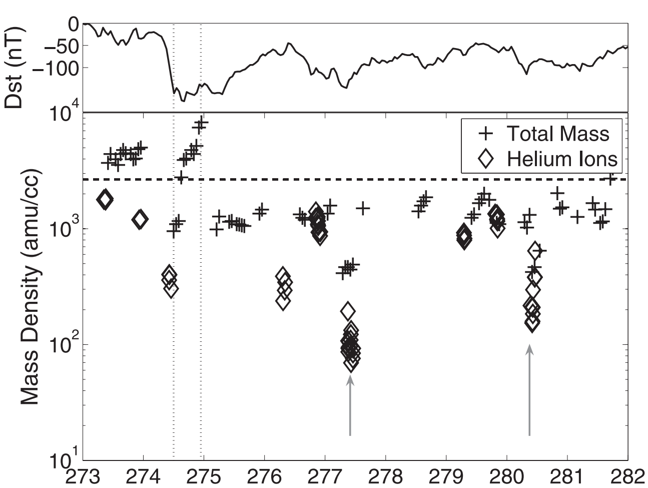

Figure 2. (top) Dst variation 30 Sep.–8 Oct. (bottom) FLR-derived total mass density and IMAGE EUV He^+ density for L = 2.5 near 4° MLON. Horizontal dashed line represents expected mass density from the *Berube et al.* (2005) model. Arrows identify plasma notches. Vertical dotted lines identify interval of enhanced mass density (see text).

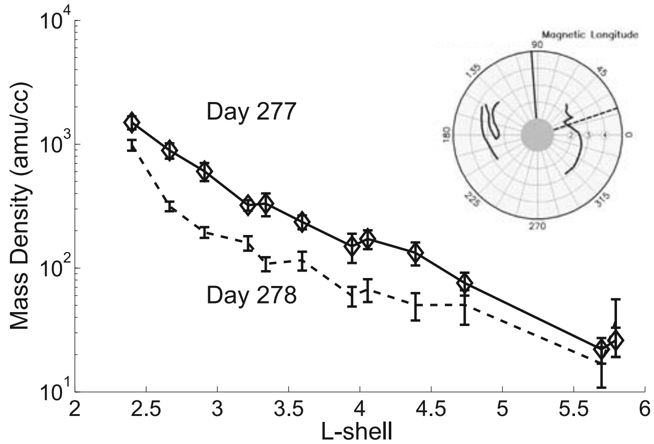

Figure 3. Mass density profiles for 08–09 UT on 4 and 5 Oct. A localized density depletion occurred on the second day. Radial solid and dashed lines across the tracer plot in the top right represent the ground station longitudes projected to the equatorial plane at these respective times.

[10] Figure 2 shows the Dst variation (Figure 2, top), and the total equatorial mass density and He^+ mass density at L = 2.5 at 4° MLON (Figure 2, bottom). Uncertainties are discussed later. The horizontal dashed line in Figure 2 (bottom) shows the heavy ion mass density predicted for L = 2.5 by the *Berube et al.* [2005] model. Several features are evident from the figure. First, the FLR-derived total mass density is significantly higher than the He^+ density, owing to the presence of protons and possibly other heavy ions. This is especially the case during the interval identified by the vertical dotted lines, when Dst was a minimum. Second, the sharp drops in total mass density and He^+ density on day 274 indicate movement of the plasmapause to L < 2.5. Subsequent densities are well below the expected plasmaspheric density (dashed line). At SAMNET (∼85° MLON) the drop in mass density occurred several UT hours earlier on this day, suggesting longitudinal structure to the plasmapause. Third, sharp order-of-magnitude depletions in total mass and He^+ density indicated by vertical arrows on days 277 and 280 identify density notches.

[11] We examine a density notch further in Figure 3. Solid and dashed curves represent FLR-derived radial mass density profiles for stations of the combined SAMNET/IMAGE arrays for 08–09 UT on 4 Oct. (day 277, no notch present) and 5 Oct. (day 288, notch). The tracer plot in the top right shows the plasmapause location at 11.00 UT on day 277. For comparison with the density profiles, radial solid and dashed lines across the tracer plot represent the SAMNET/IMAGE longitudes projected to the equatorial plane at the times shown. This was done by assuming the plasmasphere rotates at 81% of corotation (see below). The notch on 5 Oct. is associated with a plasma depletion

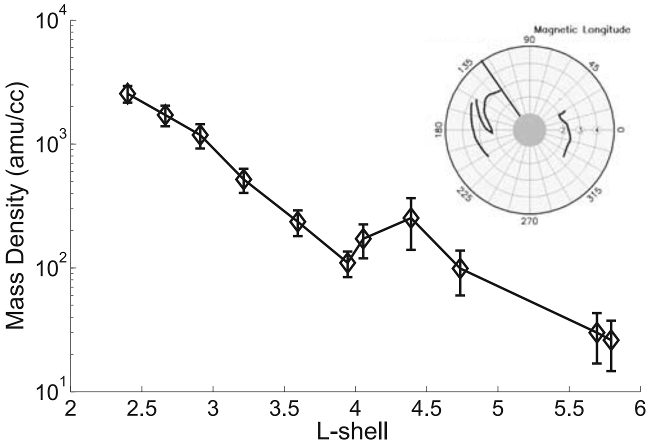

Figure 4. Mass density profile for 22–23 UT on 3 Oct. showing evidence of drainage plume around L = 4.3. The ground station longitude at this time is represented by the radial line in the tracer plot on the top right.

extending from L < 2.4 to at least L = 4.5 (well into the plasmatrough), with a maximum density decrease of order 800 amu/cc. Furthermore, the duration of the depletion signature in the FLR data and its likely rotation rate indicate that the notch is less than 4 hours wide. A similar depletion also appeared in SAMNET FLR data on day 284.2.

[12] We now examine a drainage plume in more detail. Figure 4 shows a radial mass density profile from the SAMNET/IMAGE magnetometers when the plume was overhead, at 22–23 UT on 3 Oct. The relative SAMNET/IMAGE longitude at this time is represented by the radial solid line in the tracer plot on the top right. The plasmapause is most likely near L = 3 and the increase in density near L = 4–4.5 in the density profile corresponds to the plume's passage through the plasmatrough. Note that in the tracer plot the plume's image does not quite extend to SAMNET/IMAGE longitudes.

[13] It is interesting to examine VLF whistler-derived electron densities at L = 4. These are shown in Figure 5, based on observations of natural whistlers at Halley (which maps to ~24° MLON in Figure 1). Dashed lines denote the maximum expected (i.e. with diurnal dependence removed) plasmasphere and plasmatrough electron densities from the model of *Carpenter and Anderson* [1992]. Although the plasmapause is at L < 2.5 much of this time, the whistler-derived electron densities are similar to plasmaspheric values.

4. Discussion

[14] This study has used independent ground-based and satellite imager observations to examine the temporal and spatial variation of plasma density in the inner magnetosphere during an extended disturbed period. Following *Goldstein et al.* [2005] we expect magnetospheric conditions during this period to be dominated by intervals of overshielding and sunward convection. We focus here on the plasmapause position, properties of the notch and plume, and the plasma composition.

[15] The FLR results show that the plasmapause moved to L < 2.5 late on 30 Sep. at 4° MLON and late on 1 Oct. at 85° MLON. This agrees with IMAGE EUV observations (e.g. Figure 1). Subsequent days show diurnal variations consistent with refilling effects. Occasionally FLR signatures could not be identified at SAMNET stations between L = 2.40–2.66, indicating an overhead plasmapause [*Menk et al.*, 2004]. We compared the observed plasmapause L value with several empirical models. Although the *O'Brien and Moldwin* [2003] model includes local time effects, best agreement was found with *Carpenter and Anderson*'s [1992] model.

[16] Localized density depletions (notches) appeared in all data sets. FLR observations presented in Figure 3 showed a density depletion on 5 Oct. extending from L = 2.4–4.5, while the duration of this feature suggests it spanned less than 4 hours in azimuth. Similar results were reported by *Gallagher et al.* [2005]. It is tempting to ascribe the apparent 3-day recurrence of these notches (e.g. seen in Figure 2) to a single feature rotating at around 66% of corotation. However, it is possible that a second feature formed later, for example in conjunction with the onset of southward IMF around 12 UT on 3 Oct. In that case, the FLR data suggest the first notch rotated at ~81% of corotation. This agrees with the EUV tracer observations and is the rotation rate assumed in Figures 3 and 4.

[17] Comparison of the whistler-derived densities in Figure 5 with tracer plots similar to Figure 1 shows that the whistler signals mostly did not come from features detected by the EUV experiment. The whistler ducts thus formed in regions where the He^+ density was below the EUV instrument threshold of ~40 electrons cm^{-3} [*Goldstein et al.*, 2003]. However, the relatively high whistler densities in conjunction with the EUV tracer observations suggest that at least some of the whistlers were generated in or near a drainage plume. The plume mass density profile shown in Figure 4 and the L = 4 electron densities in Figure 5 are similar to plume observations reported by *Garcia et al.* [2003] and *Kawano et al.* [2006]. However, it is difficult to equate our plume mass densities with the electron densities since the recording sites were ~30–50° apart in longitude.

[18] The combination of FLR, VLF Doppler and EUV imager techniques for the same L = 2.5 flux tube permits

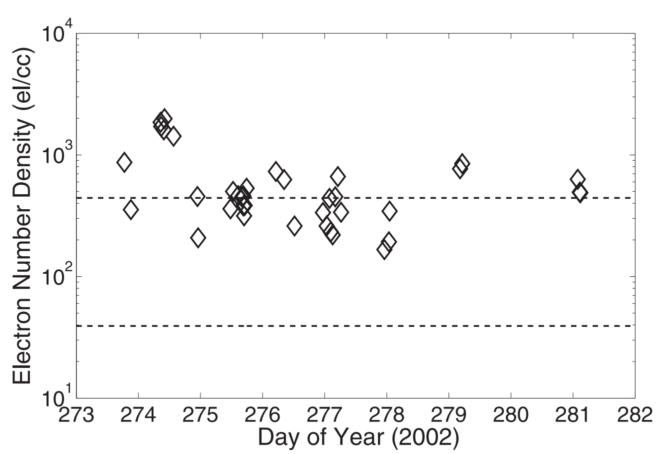

Figure 5. Whistler-derived electron density at L = 4. Dashed lines represent expected L = 4 plasmasphere (upper line) and plasmatrough density (lower line) based on the *Carpenter and Anderson* [1992] model.

Table 1. Derived Ion Number Density for Different Times During the Studied Interval[a]

		$\%H^+$		$\%He^+$		$\%O^+$	
Day	Region	Min	Max	Min	Max	Min	Max
273.40	p-sphere	56	80	18	39	−1	9
273.95	p-sphere	81	93	7	14	0	6
274.50	outer p-pause	75	90	8	16	0	7
274.90	outer p-pause	5	47	7	15	46	81
276.30	p-trough	84	95	7	14	−2	3

[a]See text for details.

estimates of the plasma composition. Suppose a neutral plasma comprises N electrons, x protons, y He^+ and z O^+ ions. N is obtained from the VLF Doppler observations, with an uncertainty of order ±10%. The He^+ ion density is inferred from the IMAGE EUV observations using the intercalibration results of *Clilverd et al.* [2003]. The uncertainty here relates to the determination of the column abundance and the equatorial abundance from this, and is around ±28% rms. The FLR measurements provide the total mass density M, with rms uncertainty of order ±10–15% [*Menk et al.*, 2004]. Writing $N = x + y + z$ and $M = xH^+ + yHe^+ + zO^+$ we can determine the H^+ and O^+ concentrations. The other main assumptions are that equatorial mass and electron density vary as R^{-3}, and that the magnetic field is dipolar. In fact, the densities are quite insensitive to the power law index [e.g., *Menk et al.*, 1999], while *Singer et al.* [1981] showed that for our L values a dipole representation introduces negligible error.

[19] By averaging groups of data points we obtained several estimates of the H^+: He^+: O^+ proportions by number. These are summarized in Table 1, where 'p-sphere' refers to the plasmasphere, and 'outer p-pause' is just outside the plasmapause, etc. In each case the range between minimum and maximum values reflects the uncertainties.

[20] With one exception, the proportions inside and outside the plasmasphere are reasonably similar, despite significant changes in total mass density (see Figure 2) and electron number density, and are similar to quiet time plasmaspheric compositions found by *Clilverd et al.* [2003]. However, just outside the plasmapause, near 22 UT on 1 Sep., the O^+ proportion by number was very high (∼60%), suggestive of an oxygen torus in that region. This interval is identified in Figure 2 by vertical dotted lines. Our observations agree with *Fraser et al.* [2005], who showed that an oxygen torus may form near the plasmapause during periods of high magnetic activity, causing heavy ion densities such as O^+ to increase by a factor of 10 or more with no concurrent variation in lighter species. Our estimated ion concentrations did not agree with predictions from the *Young et al.* [1982] model or the global core plasma model [*Gallagher et al.*, 2000]. This is perhaps not surprising when attempting to use statistical models to represent disturbed conditions.

5. Conclusions

[21] We have reported a multi-instrument study of the composition and dynamics of the plasmasphere during an extended magnetic storm. Density irregularities including notches and a drainage plume were observed with all techniques. One density depletion extended from 2.4–4.5 R_E and spanned 1–4 hours in MLT. Mass and electron densities in the plume were enhanced by a factor of ∼3. The recurrence of such features may be used to estimate the plasmasphere rotation rate; this was likely ∼81%. The combination of techniques allows the ion concentrations to be estimated. Typical H^+: He^+: O^+ proportions inside and outside the plasmasphere were of order 82:15:3% by number. However, just after the plasmapause moved Earthward of our $L = 2.5$ field line the O^+ concentration exceeded 50%, indicative of the formation of an oxygen torus. The derivation of plasmaspheric ion composition from the comparison of multiple techniques is a novel procedure which, despite the uncertainties, can provide insight into plasmaspheric dynamics.

[22] **Acknowledgments.** This work was supported by the University of Newcastle and the Australian Research Council, while the Antarctic field work was carried out under the auspices of the NERC Antarctic Funding Initiative (AFI) with logistic support from the British Antarctic Survey. Solar wind and IMF data were obtained from http://sec.noaa.gov/ace/ACErtsw_home.html and Dst from http://swdcdb.kugi.kyoto-u.ac.jp/dstdir/. This work used data from two completely independent programs both called IMAGE. Ground magnetometer data were made available by the SAMNET and IMAGE magnetometer teams. SAMNET is a PPARC National Facility operated by Lancaster University, and IMAGE is a joint European collaboration headed by the Finnish Meteorological Institute. Regarding the spacecraft data, the IMAGE Mission supported work at The University of Arizona by a subcontract under NASA contract NAS5-96020.

References

Berube, D., M. B. Moldwin, S. F. Fung, and J. L. Green (2005), A plasmaspheric mass density model and constraints on its heavy ion concentration, *J. Geophys. Res.*, *110*, A04212, doi:10.1029/2004JA010684.
Carpenter, D. L., and R. R. Anderson (1992), An ISEE/whistler model of equatorial electron density, *J. Geophys. Res.*, *97*(A2), 1097.
Clilverd, M. A., et al. (2003), In situ and ground-based intercalibration measurements of plasma density at L = 2.5, *J. Geophys. Res.*, *108*(A10), 1365, doi:10.1029/2003JA009866.
Dent, Z. C., I. R. Mann, F. W. Menk, J. Goldstein, C. R. Wilford, M. A. Clilverd, and L. G. Ozeke (2003), A coordinated ground-based and IMAGE satellite study of quiet-time plasmaspheric density profiles, *Geophys. Res. Lett.*, *30*(12), 1600, doi:10.1029/2003GL016946.
Fraser, B. J., J. L. Horwitz, J. A. Slavin, Z. C. Dent, and I. R. Mann (2005), Heavy ion mass loading of the geomagnetic field near the plasmapause and ULF wave implications, *Geophys. Res. Lett.*, *32*, L04102, doi:10.1029/2004GL021315.
Gallagher, D. L., P. D. Craven, and R. H. Comfort (2000), Global core plasma model, *J. Geophys. Res.*, *105*(A8), 18,819.
Gallagher, D. L., M. L. Adrian, and M. W. Liemohn (2005), Origin and evolution of deep plasmaspheric notches, *J. Geophys. Res.*, *110*, A09201, doi:10.1029/2004JA010906.
Garcia, L. N., S. F. Fung, J. L. Green, S. A. Boardsen, B. R. Sandel, and B. W. Reinisch (2003), Observations of the latitudinal structure of plasmaspheric convection plumes by IMAGE-RPI and EUV, *J. Geophys. Res.*, *108*(A8), 1321, doi:10.1029/2002JA009496.
Goldstein, J., M. Spasojevic, P. H. Reiff, B. R. Sandel, W. T. Forrester, D. L. Gallagher, and B. W. Reinisch (2003), Identifying the plasmapause in IMAGE EUV data using IMAGE RPI in situ steep density gradients, *J. Geophys. Res.*, *108*(A4), 1147, doi:10.1029/2002JA009475.
Goldstein, J., B. R. Sandel, W. T. Forrester, M. F. Thomsen, and M. R. Hairston (2005), Global plasmasphere evolution 22–23 April 2001, *J. Geophys. Res.*, *110*, A12218, doi:10.1029/2005JA011282.
Kawano, H., P. J. Chi, A. Kumamoto, and A. Morioka (2006), In situ observation at L = 2.3–5 by the Akebono satellite of the plasmaspheric depletion during the September 1998 magnetic storm, *J. Geophys. Res.*, *111*, A04204, doi:10.1029/2005JA011134.
Menk, F. W., D. Orr, M. A. Clilverd, A. J. Smith, C. L. Waters, and B. J. Fraser (1999), Monitoring spatial and temporal variations in the dayside plasmasphere using geomagnetic field line resonances, *J. Geophys. Res.*, *104*, 19,955.
Menk, F. W., I. R. Mann, A. J. Smith, C. L. Waters, M. A. Clilverd, and D. K. Milling (2004), Monitoring the plasmapause using geomagnetic field line resonances, *J. Geophys. Res.*, *109*, A04216, doi:10.1029/2003JA010097.

O'Brien, T. P., and M. B. Moldwin (2003), Empirical plasmapause models from magnetic indices, *Geophys. Res. Lett.*, *30*(4), 1152, doi:10.1029/2002GL016007.
Sandel, B. R., et al. (2000), The extreme ultraviolet imager investigation for the IMAGE mission, *Space Sci. Rev.*, *91*(1–2), 197.
Sandel, B. R., J. Goldstein, D. L. Gallagher, and M. Spasojevic (2003), Extreme ultraviolet imager observations of the structure and dynamics of the plasmasphere, *Space Sci. Rev.*, *109*(1–4), 25.
Singer, H. J., D. J. Southwood, R. J. Walker, and M. G. Kivelson (1981), Alfvén wave resonances in a realistic magnetospheric magnetic field geometry, *J. Geophys. Res.*, *86*, 4589.
Young, D. T., H. Balsiger, and J. Geiss (1982), Correlations of magnetospheric ion composition with geomagnetic and solar activity, *J. Geophys. Res.*, *87*(A11), 9077.

M. A. Clilverd, British Antarctic Survey, Madingley Road, Cambridge CB3 0ET, UK. (macl@bas.ac.uk)

R. S. Grew and F. W. Menk, School of Mathematical and Physical Sciences, University of Newcastle, Callaghan, NSW 2308, Australia. (russell.grew@physics.org; fred.menk@newcastle.edu.au)

B. R. Sandel, Lunar and Planetary Laboratory, University of Arizona, Tucson, AZ 85721, USA. (sandel@vega.lpl.arizona.edu)